HHS Public Access

Author manuscript

Mol Cancer Ther. Author manuscript; available in PMC 2017 May 01.

Published in final edited form as:

Mol Cancer Ther. 2016 May ; 15(5): 866–876. doi:10.1158/1535-7163.MCT-15-0729-T.

Posaconazole, a second-generation triazole antifungal drug, inhibits the Hedgehog signaling pathway and progression of basal cell carcinoma

Baozhi Chen[1,§], **Vinh Trang**[2,§], **Alex Lee**[3,†], **Noelle S. Williams**[4], **Alexandra N. Wilson**[1], **Ervin H. Epstein Jr.**[3], **Jean Y. Tang**[3,5], and **James Kim**[1,2,*]

[1]Hamon Center for Therapeutic Oncology Research, University of Texas Southwestern, Dallas, Texas 75390 USA

[2]Department of Internal Medicine, University of Texas Southwestern, Dallas, Texas 75390 USA

[3]Children's Hospital Oakland Research Institute, Oakland, CA 94609, USA

[4]Department of Biochemistry, University of Texas Southwestern, Dallas, Texas 75390 USA

[5]Department of Dermatology, Stanford University, Stanford, CA 94305, USA

Abstract

Deregulation of Hedgehog (Hh) pathway signaling has been associated with the pathogenesis of various malignancies, including basal cell carcinomas (BCC). Inhibitors of the Hh pathway currently available or under clinical investigation all bind and antagonize Smoothened (SMO), inducing a marked but transient clinical response. Tumor regrowth and therapy failure were attributed to mutations in the binding site of these small molecule SMO antagonists. The anti-fungal itraconazole was demonstrated to be a potent SMO antagonist with a distinct mechanism of action from that of current SMO inhibitors. However, itraconazole represents a suboptimal therapeutic option due to its numerous drug-drug interactions. Here we show that posaconazole, a second generation triazole anti-fungal with minimal drug-drug interactions and a favorable side effect profile, is also a potent inhibitor of the Hh pathway that functions at the level of SMO. We demonstrate that posaconazole inhibits the Hh pathway by a mechanism distinct from that of cyclopamine and other cyclopamine-competitive SMO antagonists but similar to itraconazole, has robust activity against drug-resistant SMO mutants and inhibits the growth of Hh-dependent basal cell carcinoma in vivo. Our results suggest that posaconazole, alone or in combination with other Hh pathway antagonists, may be readily tested in clinical studies for the treatment of Hh-dependent cancers.

[*]Corresponding Author: James Kim, Department of Internal Medicine, Hamon Center for Therapeutic Oncology Research, University of Texas Southwestern, 5323 Harry Hines Blvd., Dallas, Texas 75323-8593 USA; Phone: 214-648-4180; Fax: 214-648-4940; ; Email: James.Kim@UTSouthwestern.edu.

[§]Baozhi Chen and Vinh Trang contributed equally to this article.

[†]Current Address: Department of Molecular and Medical Pharmacology, University of California Los Angeles, Los Angeles, CA 90095

Conflict of Interest: E.H.E. is a founder and member of the Board of Directors for PellePharm Inc. The other authors have no conflict of interest to disclose.

Introduction

Inappropriate modulation of the Hedgehog (Hh) signaling pathway - a highly conserved, fundamental developmental pathway (1) - leads to disorders of development and cancers (1). The first cancers ascribed to defects in Hh pathway signaling were those associated with Basal cell nevus syndrome (BCNS) or Gorlin syndrome (2), an autosomal dominant disorder associated with a germline loss of one copy of *PTCH1* gene (3). Basal cell carcinoma (BCC) and medullo-blastoma are the most common tumors in these patients (2).

Under normal homeostatic conditions, the binding of a Hh ligand (SHH, IHH or DHH in mammals) (4) to Patched (PTCH), a 12-pass transmembrane protein, relieves its inhibition of Smoothened (SMO), a 7-pass transmembrane protein. SMO accumulates within the primary cilium followed by accumulation of GLI2 in the primary cilium. Once activated, GLI2 translocates into the nucleus to initiate the transcription of Hh-target genes including *PTCH1* and *GLI1* (4).

BCC is the most common cancer in the U.S. (3). For BCNS patients, BCCs arise when the second copy of PTCH is lost due to UV radiation (3). Sporadic BCC also is associated with inappropriate Hh pathway activity with ~90% and ~10% containing mutations in PTCH and SMO (3), respectively. Thus, nearly all BCC are driven by aberrant Hh pathway activation.

The strong degree of association between inappropriate Hh pathway activation and cancer suggested that abrogation of the pathway may be a viable therapeutic strategy. Cyclopamine, the first identified small molecule Hh pathway antagonist (5), binds to the SMO transmembrane domain to inhibit its activity (6). Major developmental efforts have produced numerous small molecule pathway antagonists; of which, most bind SMO near the cyclopamine-binding site despite the diversity of chemical scaffolds (7). Currently, vismodegib (GDC-0449; Genen-tech/Roche), sonidegib (NVP-LDE225; Novartis), BMS-833923 (XL139; Bristol-Myers Squibb), and LY2940680 (Lilly), and PF-04449913 (Pfizer) are being evaluated in clinical trials. However, drug resistance has emerged due to the dearth of mechanistic diversity. Resistance mechanisms include point-mutations in SMO (8-13), pathway activation downstream of SMO (10, 11, 14), and induction of alternative pathways (11).

We have previously identified itraconazole, a widely used FDA-approved systemic anti-fungal drug, as a potent inhibitor of the Hh pathway (15). Itraconazole inhibited SMO activity at a site distinct from cyclopamine and other clinically available SMO inhibitors and inhibited its accumulation in the primary cilia. Due to its distinct site of SMO antagonism, itraconazole also inhibited the activity of vismodegib- and sonidegib-resistant SMO mutants *in vitro* and *in vivo* subcutaneous and orthotopic models of murine vismodegib-resistant SMO^{D477G} medullo-blastoma (16).

Itraconazole has now been tested in several small phase II clinical trials for lung (17), prostate (18), and BCC (19) cancers. In one clinical trial, BCCs treated with a short 1-month course of itraconazole showed a significant reduction of tumor size and tumor cell proliferation that corresponded with suppression of Hh pathway activity (19).

However, itraconazole presents several challenges that limit its clinical utility. Numerous drug-drug interactions complicate its use, particularly in elderly cancer patients who often require multiple medications. Furthermore, dose adjustments are necessary for renal and hepatic insufficiencies (20).

Posaconazole, a new generation FDA-approved triazole anti-fungal and a structural analogue of itraconazole (Supplementary Fig. S1) has an excellent long-term use safety profile with mild side effects. Posaconazole has fewer drug-drug interactions than itraconazole (21) and does not require dose adjustment with mild to moderate renal or hepatic insufficiency (22).

Given the structural similarity to itraconazole and the demonstrated advantages in minimizing drug-drug interactions, we sought to investigate the ability of posaconazole to inhibit the Hh pathway, and its efficacy against Hh pathway dependent BCC.

Materials and Methods

Reagents

Posaconazole (Selleck Chemicals; S1257), voriconazole (Selleck Chemicals; S1442), vismodegib (GDC-0449; LC Laboratories), sonidegib (NVP-LDE225; LC Laboratories), and KAAD-cyclopamine (Calbiochem; 239804), SAG (Cayman Chemical; 11914) were dissolved in DMSO. Arsenic trioxide (Sigma) was formulated as previously described (16). *20(S)*-hydroxycholesterol (Steraloids Inc; C6480-000), lathosterol (Sigma), desmosterol (Sigma), and cholesterol (Sigma) were prepared in ethanol.

For *in* vivo experiments, posaconazole oral suspension (Noxafil, Merck) was obtained from the pharmacies of University of Texas Southwestern, Stanford Comprehensive Cancer Center or The Children's Hospital and Research Center at Oakland and diluted as necessary with sterile water.

Reporter-based assays

Generation and maintenance of Shh-Light2, SmoA1-Light, *Ptch*$^{-/-}$ MEFs (23) and *Smo*$^{-/-}$ fibroblast cell lines (24) have been described previously. No authentication of these cell lines was performed. Plasmid constructs for *Smo*^{WT} or drug-resistant *Smo* mutants (25), GFP, Gli-dependent firefly luciferase reporter, and TK-*Renilla* luciferase reporter (23) have been described previously. SHHN conditioned medium (CM) & HEK 293 CM (control) were collected as previously described (15) and were diluted 20-fold with the appropriate media for Hh pathway signaling assays. All reporter assays, including transient transfections, for Hh pathway activation were performed in 24 well tissue culture plates as described previously (15, 16). Luciferase units were measured on a Fluostar Optima (BMG Labtech) with dual Luciferase Assay Reporter System (Promega). GraphPad Prism software was used to generate dose response curves and IC_{50} values with four parameter logarithmic nonlinear regression fitting.

Fluorescent BOPDIPY-Cyclopamine Competition Assays

HEK293S cell line stably expressing a tetracycline inducible Smo gene has been described previously (15, 26). BODIPY-cyclopamine fluorescence was monitored using a FACScan

(Becton Dickinson) in the Moody Foundation Flow Cytometry Facility of the Children's Research Institute (UTSW). FACS data were analyzed with FlowJo software.

Immunofluorescence Imaging

NIH-3T3 cells were cultured, treated and stained with rabbit polyclonal anti-SMO (1:750 dilution) (25), mouse monoclonal anti-acetylated tubulin (1:1000 dilution, Sigma), goat anti-rabbit AlexaFluor 488 (1:667 dilution, Life Technologies) and goat anti-mouse AlexaFluor 594 (1:667 dilution, Life technologies), as previously described (15). Microscopy images were obtained by a Zeiss LSM 510 META confocal microscope in the Live Cell Imaging Core Facility (UTSW) as previously described (15).

In Vivo Studies

Pharmacokinetic Study

Please see Supplemental Information for full methods of the pharmacokinetic study. All studies were approved by and conformed to the policies and regulations of Institutional Animal Care and Use Committees (IACUC) at UTSW. Mice were maintained in a standard facility and conditions of a 12 h light/dark cycle, temperature and humidity at University of Texas Southwestern (UTSW). Mice were administered 1 dose of posaconazole (Noxafil, Merck) 30 mg/kg or 60 mg/kg by oral gavage and sacrificed at various time points. Drinking water was acidified (pH 2.5). Plasma was isolated from whole blood by centrifugation, treated with methanol containing formic acid and tolbutamide internal standard, and subsequent supernatant used for posaconazole measurement. An AB Sciex (Framingham, MA) 3200 Qtrap mass spectrometer coupled to a Shimadzu (Columbia, MD) Prominence LC with an Agilent (Santa Clara, CA) XDB C18 chromatography column was used to detect posaconazole levels. Pharmacokinetic parameters were calculated using the noncompartmental analysis tool in Phoenix WinNonlin (Certara Corp, Princeton, NJ.)

Drug Treatment Study

Mice were kept at standard conditions of a 12 h light/dark cycle, temperature and humidity at the Children's Hospital Oakland Research Institute (CHORI). All of the studies were approved by and conformed to the policies and regulations of the IACUC at CHORI. Autochthonous BCC tumors from *Ptch1*$^{+/-}$;*K14*$^{CreER2/+}$;*Trp53*$^{fl/fl}$ mice (27) were obtained as described previously (16) and digested to a single cell suspension with 0.5% Collagenase 1 (Life Technologies) in HBSS solution. The suspension was mixed 1:1 with Matrigel (Fisher Scientific) and injected subcutaneously into two distinct dorsal sites of NOD/SCID mice (Jackson Laboratories). When BCCs were between 5-10 mm in diameter, mice were treated with vehicle control or posaconazole 30 or 60 mg/kg via oral gavage twice daily on weekdays and once daily on weekend. At the end of the experiment, mice were euthanized and tumor samples were collected.

Necrosis Scoring of BCC tumors—Scoring of H&E sections of BCC tumors after the drug treatment study have been described previously (15). Necrosis was scored as follows: 0 = No evidence of necrosis with large basaloid cells; 1 = mild necrosis with nuclear pyknosis; 2 = moderate necrosis with <25% necrosis; 3 = severe necrosis with > 25% necrosis.

Comparison between cyclodextrin control and posaconazole treated tumors were made using a two-sided unpaired *t*-test with GraphPad Prism software.

Quantitative PCR of *Gli1* Transcript in Basal Cell Carcinoma Cells and Allografts—Generation and maintenance of BCC cell lines, ASZ and BSZ, have been previously described (28). No authentication of these cell lines was performed. After confluence, BCC cells were treated with drugs for 2 days in growth medium except with 0.5% chelexed FBS. For BCC allograft tumors, tissue was collected 4 hours after the last dose of drug and flash frozen in liquid nitrogen. Tumors were mechanically homogenized with a Minibeadbeater (Biospec Product). Preparation of total RNA and cDNA have been described previously (15). *Gli1* mRNA was quantified using Bio-Rad CFX real-time cycler with SYBR (Bio-Rad) as previously described(16). Data are presented as fold induction relative to control samples using the ΔΔCt ($2^{-\Delta\Delta Ct}$) method with *Hprt1* as an internal control gene.

Primers:

Gli1:

Forward: 5’ AAGGAATTCGTGTGCCATTGGG

Reverse: 5’ ACATGTAAGGCTTCTCACCCGT

Hprt1:

Forward: 5’ CGTGATTAGCGATGATGAACCAGG

Reverse: 5’ CATCTCGAGCAAGTCTTTCAGTCC

Results

Posaconazole’s effect on Hh pathway activity was tested using SHH-Light2 cells, a clonal NIH-3T3 cell line stably expressing an 8x-Gli binding site-luciferase reporter (23). Posaconazole potently inhibited SHHN conditioned medium (CM) (29) induced Hh pathway activation in a dose-dependent manner with an IC_{50} of 880 nM (Fig. 1A). In contrast, voriconazole, another triazole antifungal drug (Supplementary Fig. S1) with a contrasting chemical backbone, did not demonstrate any detectable inhibition of the Hh pathway up to 40 μM.

Posaconazole inhibits antifungal growth by its potent antagonism of 14-α-lanosterol demethylase (14LDM), an enzyme required for ergosterol biosynthesis in fungi and cholesterol biosynthesis in mammals (30). HMG-CoA reductase antagonists that inhibit cholesterol biosynthesis upstream of 14LDM have been shown to inhibit Hh reception between PTCH and SMO in cells treated with cyclodextrin to deplete cellular sterols (31). We tested whether posaconazole’s inhibition of 14LDM in cholesterol biosynthesis may account for its ability to inhibit Hh pathway activation. Addition of 25 μM each of cholesterol, lathosterol, and desmosterol – components of cholesterol biosynthesis downstream of 14LDM – to posaconazole and SHHN was unable to reverse the inhibitory effect of posaconazole (Fig. 1B). Cholesterol, lathosterol, and desmosterol alone were insufficient to induce Hh pathway activation in Shh-Light2 cells (Fig. 1C). These results

suggest that posaconazole inhibits the Hh pathway by a mechanism distinct from its antifungal inhibitory activity of 14LDM.

Next, we mapped posaconazole's inhibitory effect on the pathway. Constitutively active *Ptch*$^{-/-}$ murine embryonic fibroblast cells (23) were transiently transfected with an 8x-Gli luciferase reporter and treated with increasing concentrations of posaconazole. Posaconazole inhibited the Hh pathway with an IC_{50} of 986 nM (Fig. 2A), similar to SHH-Light2 cells (Fig. 1A). In contrast, posaconazole had no inhibitory effect in Shh-Light2 *SmoA1* cells that stably expressed the constitutively active SMOA1 (SMO^{W539L}) mutant (23) (Fig. 2B).

Results presented thus far suggested that posaconazole acted downstream of PTCH and at or upstream of SMO in the pathway. To determine if posaconazole binds directly to SMO, we tested whether it could compete with cyclopamine, an alkaloid that binds to the transmembrane domain of SMO and inhibits its activity (6). Tetracycline inducible, SMO-expressing HEK-293 cells (26) were treated with a fluorescently labeled BODIPY-cyclopamine (6) and varying concentrations of KAAD-cyclopamine or posaconazole (Fig. 2C,D). BODIPY fluorescence was measured by flow cytometry. SMO-induced cells treated with BODIPY-cyclopamine (BD) 5 nM showed ~10-fold increase in fluorescence over uninduced cells (no tetracycline treatment) (Fig. 2C). The increase in fluorescence of uninduced cells with BD from uninduced cells with no BD was most likely due to non-specific binding of BD (Fig. 2C). The addition of KAAD-cyclopamine 200 nM and 400 nM (~10x- and 20x-IC_{50}, respectively), a more potent derivative of cyclopamine (23), to BD treated SMO-overexpressing cells reduced the fluorescence of BD bound to SMO to baseline levels (Fig. 2D), reflecting the competition of KAAD-cyclopamine and BD for binding to SMO (Fig. 2D). However, the addition of increasing concentrations of posaconazole, up to 10 μM (~11x IC_{50}), did not significantly decrease the fluorescence of BODIPY-cyclopamine bound to SMO (Fig. 2E). These results suggest that posaconazole does not bind to SMO at the same site as cyclopamine.

To further verify that posaconazole did not bind to SMO in the same binding region as cyclopamine, Hh pathway activity was induced with SAG, a small molecule SMO agonist that competes with cyclopamine for binding (32), and competed with KAAD-cyclopamine or posaconazole (Fig. 3A, B). Titration of SAG with increasing concentrations of KAAD-cyclopamine from 0 to 100 nM (5x IC_{50}) shifted the EC_{50} of SAG more than 7-fold from 34 nM to 244 nM (Fig. 3A) while maintaining similar levels of maximal pathway activation. These results suggested that KAAD-cyclopamine and SAG compete with each other for SMO binding. In contrast, increasing concentrations of posaconazole from 0 to 7.5 μM (8.5x IC_{50}) did not significantly alter the EC_{50} of SAG but rather significantly decreased the maximal induction of pathway activation (Fig. 3B). These results suggested that posaconazole does not compete with SAG for SMO binding and acts as a non-competitive inhibitor of SAG.

20(S)-hydroxycholesterol has been shown to activate the Hh signaling pathway(26, 33) by binding to the N-terminal extracellular cysteine rich domain (CRD) of SMO (34-36) and act non-competitively with itraconazole(37). Titration of *20(S)*-hydroxycholesterol with increasing concentrations of posaconazole did not significantly alter the EC_{50} of the

oxysterol (Fig. 3C), similar to SAG (Fig. 3B). Conversely, titration of posaconazole with increasing concentrations of *20(S)*-hydroxycholesterol did not significantly alter the IC_{50} of posaconazole (Fig. 3D). Similar to itraconazole (15), posaconazole inhibited pathway activation by *20(S)*-hydroxycholesterol (164 nM; Fig. 3C) with much greater potency than SHHN (880 nM; Fig. 1A). These results suggested that posaconazole is a non-competitive inhibitor of *20(S)*-hydroxycholesterol and binds to a target distinct from the CRD of SMO.

As posaconazole did not appear to bind to SMO at the same site as KAAD-cyclopamine, we tested whether the combination of posaconazole and cyclopamine may act synergistically. Indeed, titration of posaconazole with increasing concentrations of KAAD-cyclopamine diminished the IC_{50} of posaconazole ~2.5 fold (Fig. 3E) suggesting that posaconazole and KAAD-cyclopamine act synergistically to inhibit the Hh pathway. Treatment of SHH-Light2 cells activated by SHHN CM with subtherapeutic doses of posaconazole 1 μM (~1.1x IC_{50}), KAAD-cyclopamine 10 nM (~0.5x IC_{50}) or vismodegib (GDC-0449) 20 nM (~1x IC_{50}), a cyclopamine-competitive SMO antagonist, partially inhibited the Hh pathway (Fig. 3F). However, the combination of posaconazole with either KAAD-cyclopamine or vismodegib at the same subtherapeutic doses completely inhibited Hh pathway activation (Fig. 3F). We also tested subtherapeutic doses of posaconazole in combination with KAAD-cyclopamine or vismodegib (Fig. 3G) on constitutively active ASZ and BSZ basal cell carcinoma cells (28) that were derived from $Ptch^{+/-}$ and $Ptch^{+/-};K14^{CreER/+};Trp53^{fl/fl}$ murine BCC, respectively. Similar to the results in SHH-Light2 cells (Fig. 3F), combination of drugs inhibited pathway activation more completely than single drugs alone. These results confirmed the cooperativity of posaconazole and cyclopamine-competitive SMO antagonists and that indeed, posaconazole acted upon SMO at a distinct site from the cyclopamine-binding site.

As posaconazole did not compete with SMO agonists and antagonists that are known to bind SMO, we wondered if posaconazole may act on SMO by disruption of its localization in the primary cilium. Localization and accumulation of SMO in the primary cilia have been observed upon pathway activation whether by Hh ligands, SMO agonists, or constitutively-active mutant SMO (25, 38, 39). With the addition of posaconazole to SHHN induced NIH-3T3 cells, a marked decrease in the ciliary accumulation of SMO was seen (Fig. 4) from ~87% of cilia in SHHN and vehicle control treated cells to ~16% of primary cilia in SHHN and posaconazole treated cells ($p < 0.0001$). Control cells treated with vehicle control alone (without SHHN) showed ~8% of primary cilia with SMO (Fig. 4B). These results correlated well with the degree of pathway inhibition by posaconazole suggesting that posaconazole acts on the pathway by a net decrease in the accumulation of SMO in primary cilia to activate the pathway.

Single, weight based oral administration of posaconazole 30 mg/kg or 60 mg/kg resulted in pharmacokinetic profiles (Fig. 5A, Supplementary Table S1) similar to those reported previously in mice (40). Doubling the posaconazole dose from 30 mg/kg to 60 mg/kg did not substantially increase the maximal plasma concentration (C_{max}) from 16.1 μg/ml to 15.9 μg/ml, respectively, or the $AUC_{0\text{-}24h}$ from 244.65 μg*hr/ml to 288.46 μg*hr/ml, respectively (Fig. 5A, Supplementary Table 1). Thus, analogous to human studies (41), the absorption of posaconazole from the murine intestine is limited beyond 30 mg/kg.

To evaluate the therapeutic efficacy of posaconazole to treat Hh-dependent tumors, we treated nude mice bearing subcutaneous allografts of murine *Ptch*$^{+/-}$;*p53*$^{-/-}$ BCC (42) with posaconazole 30 mg/kg or 60 m/kg twice-daily. Posaconazole treatment significantly suppressed tumor growth (Fig. 5B) compared to vehicle control treated tumors ($p < 0.005$). In a separate experiment, allografted BCC tumors treated with posaconazole showed significant inhibition of the Hh pathway as measured by *Gli1* mRNA (Fig. 5C). The similar degrees of tumor growth suppression and Hh pathway inhibition between posaconazole 30 mg/kg and 60 m/kg were consistent with the results of our pharmacokinetic study that showed the 60 mg/kg dose did not substantially increase plasma posaconazole levels. Microscopic examination of tumor samples treated with posaconazole showed significant levels of necrosis that were not present in tumors treated with vehicle control (Fig. 5D, E), as evidenced by the architectural destruction of tumor cell nests and surrounding stroma (Fig. 5E).

Recently, several mechanisms of resistance (8-13) to cyclopamine-competitive antagonists, vismodegib (GDC-0445) and sonidegib (NVP-LDE225) (43, 44), have emerged. As our data suggested that posaconazole does not bind to the cyclopamine-binding region of SMO, we examined the ability of posaconazole with or without arsenic trioxide (ATO), an inhibitor of GLI proteins (25), to inhibit the Hh pathway in SMO mutants with demonstrated resistance to the vismodegib (D477G, E522K) and sonidegib (G457S, S392N, D388N, N223D, L225R). *Smo*$^{-/-}$ murine fibroblasts were transiently transfected with wild-type (WT) or drug-resistant *Smo* mutants and stimulated with SHHN CM. Vismodegib- and sonidegib-resistant SMO mutants were resistant to vismodegib 0.5 μM (~40x IC_{50}) and sonidegib 0.5 μM (~80x IC_{50}) treatment, respectively (Supplementary Fig. S2). SMO-G457S was inhibited by sonidegib 0.5 μM but was resistant at lower dose of 0.05 μM, consistent with previous reports (10). Posaconazole showed inhibitory activity against all of the tested drug-resistant SMO mutants (Fig. 6). The combination of posaconazole and ATO further inhibited the activity of drug-resistant SMO mutants (Fig. 6).

Discussion

Similar to itraconazole (15, 16), posaconazole inhibited the Hh pathway downstream of PTCH and at or upstream of SMO, did not compete with cyclopamine, SAG, or *20(S)*-hydroxycholesterol for SMO binding, inhibited SMO accumulation in the primary cilia, had inhibitory activity against drug-resistant SMO mutants and inhibited the growth of Hh-dependent BCC.

Our results from the drug competition experiments (Fig. 3A-D) suggest that posaconazole interacts with SMO in a region distinct from the N-terminal CRD (where oxysterols bind) (34-36), and the cyclopamine-binding regions of the transmembrane domain, where all of the current clinically tested SMO inhibitors bind (7). Alternatively, as posaconazole is a highly hydrophobic molecule, it may interact with the SMO transmembrane domains to disrupt the multimerization of SMO (45, 46); an event that occurs when Hh binds to PTCH (45) and may be required for SMO function. A third possibility may be that posaconazole does not bind SMO directly but rather, binds to an upstream target that mediates SMO action, particularly its localization to the primary cilia.

Itraconazole has shown activity in human clinical trials against several tumor types including Hh-dependent BCC (19). However, itraconazole and its primary metabolite, hydroxy-itraconazole, are both strong inhibitors and substrates of the major drug metabolizing enzyme, cytochrome P450 (CYP) 3A4 (47, 48), and weaker inhibitors of CYP2C9 and CYP2C19 (49). Thus, itraconazole has numerous drug-drug interactions that lead to toxicities resulting in frequent dose adjustments or discontinuation. Also, itraconazole requires dose adjustments in the setting of renal and hepatic insufficiencies (21). Posaconazole, in contrast, is metabolized by uridine diphosphateglucuronosyltransferase enzyme pathways (50). Posaconazole inhibits CYP3A4 but does not inhibit other drug metabolizing isoenzymes CYP 1A2, 2C8, 2C9, 2D6, or 2E1 (51). Thus, posaconazole has a decreased potential for drug-drug interactions compared to itraconazole. Posaconazole also does not require dose adjustments for renal and hepatic insufficiencies (22). Posaconazole treatments lasting up to two years without significant adverse events has been reported (22, 52); an important consideration as continuous, prolonged courses of therapy will most likely be needed for cancer treatment.

Plasma C_{max} and $AUC_{0\text{-}24h}$ at 30 mg/kg in our murine pharmacokinetic study are ~12x and ~5x higher, respectively, than those reported for 800 mg single dose in humans (41) while half-life was shorter by ~7 hrs. However, the patients in the human study (41) did not take posaconazole with an acidic drink as in our murine study. Acidification of the stomach may double the plasma C_{max} and $AUC_{0\text{-}24h}$ (53) and thus, bring human posaconazole levels closer in range to those seen in our murine study.

Response of human BCC to posaconazole may require less drug than the doses administered here. Our preclinical itraconazole study (15) suggested that at least 800 mg/day of itraconazole may be required for tumor responses in patients. However, in our phase II clinical trial, human BCC responded with itracon-azole 400 mg/day (19), half the dose of our preclinical studies. Analogously, human BCC may show similar responses with lower doses of posaconazole than those reported here.

Recently, we and others (12, 13) have shown that the majority of human vismodegib-resistant BCCs are due to two classes of SMO mutations in the transmembrane domain: (i) those within or adjacent to the vismodegib binding pocket that require upstream inactivation of PTCH (either by mutation or Hh lig-and) for activation and (ii) mutations far from the binding site that confer constitutive SMO activity. Given our results in the present study (Fig. 2B and 6), we predict that posaconazole will have activity against the first class of SMO mutants but not against the second class of mutants that confer constitutive SMO activity. However, we have shown that a combination of posaconazole and cyclopamine-competitive antagonists acts synergistically to suppress SMO activation (Fig. 3E-G). Initial use of posaconazole with a cyclopamine-competitive antagonist may provide a more potent, durable response with suppression or delay of resistant tumors than with a cyclopamine-competitive antagonist alone. Alternatively, combination of posaconazole and arsenic trioxide (Fig. 6) may provide durable responses without the appearance of drug-resistant SMO mutants due to inhibition of downstream GLI transcription factors by ATO.

The limited mechanistic diversity of current cyclopamine-competitive SMO antagonists has led to the emergence of drug-resistant SMO mutants (8-13). Posaconazole has been studied for nearly 20 years, has been FDA-approved since 2006 with well-known toxicities, has a favorable drug-drug interaction profile, and inhibits SMO with a distinct mechanism from current SMO antagonists that are under clinical investigation. Thus, posaconazole, either alone or in combination with other Hh antagonists, offers readily available therapeutic strategies that can be tested immediately in human trials against Hh-dependent cancers.

Supplementary Material

Refer to Web version on PubMed Central for supplementary material.

Acknowledgments

We thank Dr. Lawrence Lum for his helpful comments and discussions of the manuscript.

Financial Support: This research was supported in part by grants to N.S. Williams and the Preclinical Pharmacology Core from Cancer Prevention Research Institute of Texas (RP11078-C3) and the UTSW Institute for Innovations in Medical Technology (IIMT), to J.Y. Tang from the Damon Runyon Cancer Research Foundation (Clinical Investigator Award), to E.H. Epstein Jr. from National Institutes of Health (5R01CA163611), and to J. Kim from Free to Breathe (Young Investigator Research Grant), Bonnie J. Addario Lung Cancer Foundation (Young Investigator Award), UT Southwestern - American Cancer Society Institutional Research Grant and UT Southwestern institutional funds.

References

1. Barakat MT, Humke EW, Scott MP. Learning from Jekyll to control Hyde: Hedgehog signaling in development and cancer. Trends Mol Med. 2010; 16:337–48. [PubMed: 20696410]
2. Gorlin RJ. Nevoid basal-cell carcinoma syndrome. Medicine (Baltimore). 1987; 66:98–113. [PubMed: 3547011]
3. Epstein EH. Basal cell carcinomas: attack of the hedgehog. Nat Rev Cancer. 2008; 8:743–54. [PubMed: 18813320]
4. Sasai N, Briscoe J. Primary cilia and graded Sonic Hedgehog signaling. Wiley Interdiscip Rev Dev Biol. 2012; 1:753–72. [PubMed: 23799571]
5. Cooper MK, Porter JA, Young KE, Beachy PA. Teratogen-mediated inhibition of target tissue response to Shh signaling. Science. 1998; 280:1603–7. [PubMed: 9616123]
6. Chen JK, Taipale J, Cooper MK, Beachy PA. Inhibition of Hedgehog signaling by direct binding of cyclopamine to Smoothened. Genes Dev. 2002; 16:2743–8. [PubMed: 12414725]
7. Sharpe HJ, Wang W, Hannoush RN, de Sauvage FJ. Regulation of the oncoprotein Smoothened by small molecules. Nat Chem Biol. 2015; 11:246–55. [PubMed: 25785427]
8. Rudin CM, Hann CL, Laterra J, Yauch RL, Callahan CA, Fu L, et al. Treatment of medulloblastoma with hedgehog pathway inhibitor GDC-0449. New Engl J Med. 2009; 361:1173–8. [PubMed: 19726761]
9. Yauch RL, Dijkgraaf GJ, Alicke B, Januario T, Ahn CP, Holcomb T, et al. Smoothened mutation confers resistance to a Hedgehog pathway inhibitor in medulloblastoma. Science. 2009; 326:572–4. [PubMed: 19726788]
10. Buonamici S, Williams J, Morrissey M, Wang A, Guo R, Vattay A, et al. Interfering with resistance to smoothened antagonists by inhibition of the PI3K pathway in medulloblastoma. Sci Transl Med. 2010; 2:51ra70.
11. Dijkgraaf GJ, Alicke B, Weinmann L, Januario T, West K, Modrusan Z, et al. Small molecule inhibition of GDC-0449 refractory smoothened mutants and downstream mechanisms of drug resistance. Cancer Res. 2011; 71:435–44. [PubMed: 21123452]

12. Sharpe HJ, Pau G, Dijkgraaf GJ, Basset-Seguin N, Modrusan Z, Januario T, et al. Genomic analysis of smoothened inhibitor resistance in Basal cell carcinoma. Cancer Cell. 2015; 27:327–41. [PubMed: 25759019]
13. Atwood SX, Sarin KY, Whitson RJ, Li JR, Kim G, Rezaee M, et al. Smoothened variants explain the majority of drug resistance in Basal cell carcinoma. Cancer Cell. 2015; 27:342–53. [PubMed: 25759020]
14. Atwood SX, Li M, Lee A, Tang JY, Oro AE. GLI activation by atypical protein kinase C iota/lambda regulates the growth of basal cell carcinomas. Nature. 2013; 494:484–8. [PubMed: 23446420]
15. Kim J, Tang JY, Gong R, Kim J, Lee JJ, Clemons KV, et al. Itraconazole, a commonly used antifungal that inhibits Hedgehog pathway activity and cancer growth. Cancer Cell. 2010; 17:388–99. [PubMed: 20385363]
16. Kim J, Aftab BT, Tang JY, Kim D, Lee AH, Rezaee M, et al. Itraconazole and arsenic trioxide inhibit Hedgehog pathway activation and tumor growth associated with acquired resistance to smoothened antagonists. Cancer Cell. 2013; 23:23–34. [PubMed: 23291299]
17. Rudin CM, Brahmer JR, Juergens RA, Hann CL, Ettinger DS, Sebree R, et al. Phase 2 study of pemetrexed and itraconazole as second-line therapy for metastatic nonsquamous non-small-cell lung cancer. J Thorac Oncol. 2013; 8:619–23. [PubMed: 23546045]
18. Antonarakis ES, Heath EI, Smith DC, Rathkopf D, Blackford AL, Danila DC, et al. Repurposing itraconazole as a treatment for advanced prostate cancer: a noncomparative randomized phase II trial in men with metastatic castration-resistant prostate cancer. Oncologist. 2013; 18:163–73. [PubMed: 23340005]
19. Kim DJ, Kim J, Spaunhurst K, Montoya J, Khodosh R, Chandra K, et al. Open-Label, Exploratory Phase II Trial of Oral Itraconazole for the Treatment of Basal Cell Carcinoma. J Clin Oncol. 2014
20. Lass-Florl C. Triazole antifungal agents in invasive fungal infections: a comparative review. Drugs. 2011; 71:2405–19. [PubMed: 22141384]
21. Katragkou A, Tsikopoulou F, Roilides E, Zaoutis TE. Posaconazole: when and how? The clinician's view. Mycoses. 2012; 55:110–22. [PubMed: 21762211]
22. Raad II, Graybill JR, Bustamante AB, Cornely OA, Gaona-Flores V, Afif C, et al. Safety of long-term oral posaconazole use in the treatment of refractory invasive fungal infections. Clin Infect Dis. 2006; 42:1726–34. [PubMed: 16705579]
23. Taipale J, Chen JK, Cooper MK, Wang B, Mann RK, Milenkovic L, et al. Effects of oncogenic mutations in Smoothened and Patched can be reversed by cyclopamine. Nature. 2000; 406:1005–9. [PubMed: 10984056]
24. Varjosalo M, Li SP, Taipale J. Divergence of hedgehog signal transduction mechanism between Drosophila and mammals. Dev Cell. 2006; 10:177–86. [PubMed: 16459297]
25. Kim J, Lee JJ, Kim J, Gardner D, Beachy PA. Arsenic antagonizes the Hedgehog pathway by preventing ciliary accumulation and reducing stability of the Gli2 transcriptional effector. Proc Natl Acad Sci U S A. 2010; 107:13432–7. [PubMed: 20624968]
26. Dwyer JR, Sever N, Carlson M, Nelson SF, Beachy PA, Parhami F. Oxysterols are novel activators of the hedgehog signaling pathway in pluripotent mesenchymal cells. J Biol Chem. 2007; 282:8959–68. [PubMed: 17200122]
27. Tang JY, Xiao TZ, Oda Y, Chang KS, Shpall E, Wu A, et al. Vitamin D3 inhibits hedgehog signaling and proliferation in murine Basal cell carcinomas. Cancer Prev Res. 2011; 4:744–51.
28. So PL, Langston AW, Daniallinia N, Hebert JL, Fujimoto MA, Khaimskiy Y, et al. Long-term establishment, characterization and manipulation of cell lines from mouse basal cell carcinoma tumors. Exp Dermatol. 2006; 15:742–50. [PubMed: 16881970]
29. Maity T, Fuse N, Beachy PA. Molecular mechanisms of Sonic hedgehog mutant effects in holoprosencephaly. Proc Natl Acad Sci U S A. 2005; 102:17026–31. [PubMed: 16282375]
30. Lepesheva GI, Waterman MR. Sterol 14alpha-demethylase cytochrome P450 (CYP51), a P450 in all biological kingdoms. Biochim Biophys Acta. 2007; 1770:467–77. [PubMed: 16963187]
31. Cooper MK, Wassif CA, Krakowiak PA, Taipale J, Gong R, Kelley RI, et al. A defective response to Hedgehog signaling in disorders of cholesterol biosynthesis. Nat Genet. 2003; 33:508–13. [PubMed: 12652302]

32. Chen JK, Taipale J, Young KE, Maiti T, Beachy PA. Small molecule modulation of Smoothened activity. Proc Natl Acad Sci U S A. 2002; 99:14071–6. [PubMed: 12391318]
33. Corcoran RB, Scott MP. Oxysterols stimulate Sonic hedgehog signal transduction and proliferation of medulloblastoma cells. Proc Natl Acad Sci U S A. 2006; 103:8408–13. [PubMed: 16707575]
34. Nedelcu D, Liu J, Xu Y, Jao C, Salic A. Oxysterol binding to the extracellular domain of Smoothened in Hedgehog signaling. Nat Chem Biol. 2013; 9:557–64. [PubMed: 23831757]
35. Myers BR, Sever N, Chong YC, Kim J, Belani JD, Rychnovsky S, et al. Hedgehog pathway modulation by multiple lipid binding sites on the smoothened effector of signal response. Dev Cell. 2013; 26:346–57. [PubMed: 23954590]
36. Nachtergaele S, Whalen DM, Mydock LK, Zhao Z, Malinauskas T, Krishnan K, et al. Structure and function of the Smoothened extracellular domain in vertebrate Hedgehog signaling. eLife. 2013; 2:e01340. [PubMed: 24171105]
37. Nachtergaele S, Mydock LK, Krishnan K, Rammohan J, Schlesinger PH, Covey DF, et al. Oxysterols are allosteric activators of the oncoprotein Smoothened. Nat Chem Biol. 2012; 8:211–20. [PubMed: 22231273]
38. Corbit KC, Aanstad P, Singla V, Norman AR, Stainier DY, Reiter JF. Vertebrate Smoothened functions at the primary cilium. Nature. 2005; 437:1018–21. [PubMed: 16136078]
39. Rohatgi R, Milenkovic L, Scott MP. Patched1 regulates hedgehog signaling at the primary cilium. Science. 2007; 317:372–6. [PubMed: 17641202]
40. Nomeir AA, Kumari P, Hilbert MJ, Gupta S, Loebenberg D, Cacciapuoti A, et al. Pharmacokinetics of SCH 56592, a new azole broad-spectrum antifungal agent, in mice, rats, rabbits, dogs, and cynomolgus monkeys. Antimicrob Agents Chemother. 2000; 44:727–31. [PubMed: 10681346]
41. Courtney R, Pai S, Laughlin M, Lim J, Batra V. Pharmacokinetics, safety, and tolerability of oral posaconazole administered in single and multiple doses in healthy adults. Antimicrob Agents Chemother. 2003; 47:2788–95. [PubMed: 12936975]
42. Xiao TZ, Tang JY, Wu A, Shpall E, Khaimsky I, So P, Epstein EH Jr. Hedgehog signaling of BCC is inhibited by Vitamin D: Implication for a chemopreventive agent against BCC carcinogenesis. J Invest Dermatol. 2009; 129:S32.
43. Robarge KD, Brunton SA, Castanedo GM, Cui Y, Dina MS, Goldsmith R, et al. GDC-0449-a potent inhibitor of the hedgehog pathway. Bioorg Med Chem Lett. 2009; 19:5576–81. [PubMed: 19716296]
44. Pan S, Wu X, Jiang J, Gao W, Wan Y, Cheng D, et al. Discovery of NVP-LDE225, a Potent and Selective Smoothened Antagonist. ACS Med Chem Lett. 2010; 1:130–4. [PubMed: 24900187]
45. Zhao Y, Tong C, Jiang J. Hedgehog regulates smoothened activity by inducing a conformational switch. Nature. 2007; 450:252–8. [PubMed: 17960137]
46. Wang C, Wu H, Katritch V, Han GW, Huang XP, Liu W, et al. Structure of the human smoothened receptor bound to an antitumour agent. Nature. 2013; 497:338–43. [PubMed: 23636324]
47. Isoherranen N, Kunze KL, Allen KE, Nelson WL, Thummel KE. Role of itraconazole metabolites in CYP3A4 inhibition. Drug Metab Dispos. 2004; 32:1121–31. [PubMed: 15242978]
48. Templeton IE, Thummel KE, Kharasch ED, Kunze KL, Hoffer C, Nelson WL, et al. Contribution of itraconazole metabolites to inhibition of CYP3A4 in vivo. Clin Pharmacol Ther. 2008; 83:77–85. [PubMed: 17495874]
49. Niwa T, Shiraga T, Takagi A. Effect of antifungal drugs on cytochrome P450 (CYP) 2C9, CYP2C19, and CYP3A4 activities in human liver microsomes. Biol Pharm Bull. 2005; 28:1805–8. [PubMed: 16141567]
50. Ghosal A, Hapangama N, Yuan Y, Achanfuo-Yeboah J, Iannucci R, Chowdhury S, et al. Identification of human UDP-glucuronosyltransferase enzyme(s) responsible for the glucuronidation of posaconazole (Noxafil). Drug metabolism and disposition: the biological fate of chemicals. 2004; 32:267–71. [PubMed: 14744950]
51. Wexler D, Courtney R, Richards W, Banfield C, Lim J, Laughlin M. Effect of posaconazole on cytochrome P450 enzymes: a randomized, open-label, two-way crossover study. European journal of pharmaceutical sciences : official journal of the European Federation for Pharmaceutical Sciences. 2004; 21:645–53. [PubMed: 15066665]

52. Anstead GM, Corcoran G, Lewis J, Berg D, Graybill JR. Refractory coccidioidomycosis treated with posaconazole. Clin Infect Dis. 2005; 40:1770–6. [PubMed: 15909265]

53. Krishna G, Moton A, Ma L, Medlock MM, McLeod J. Pharmacokinetics and absorption of posaconazole oral suspension under various gastric conditions in healthy volunteers. Antimicrob Agents Chemother. 2009; 53:958–66. [PubMed: 19075045]

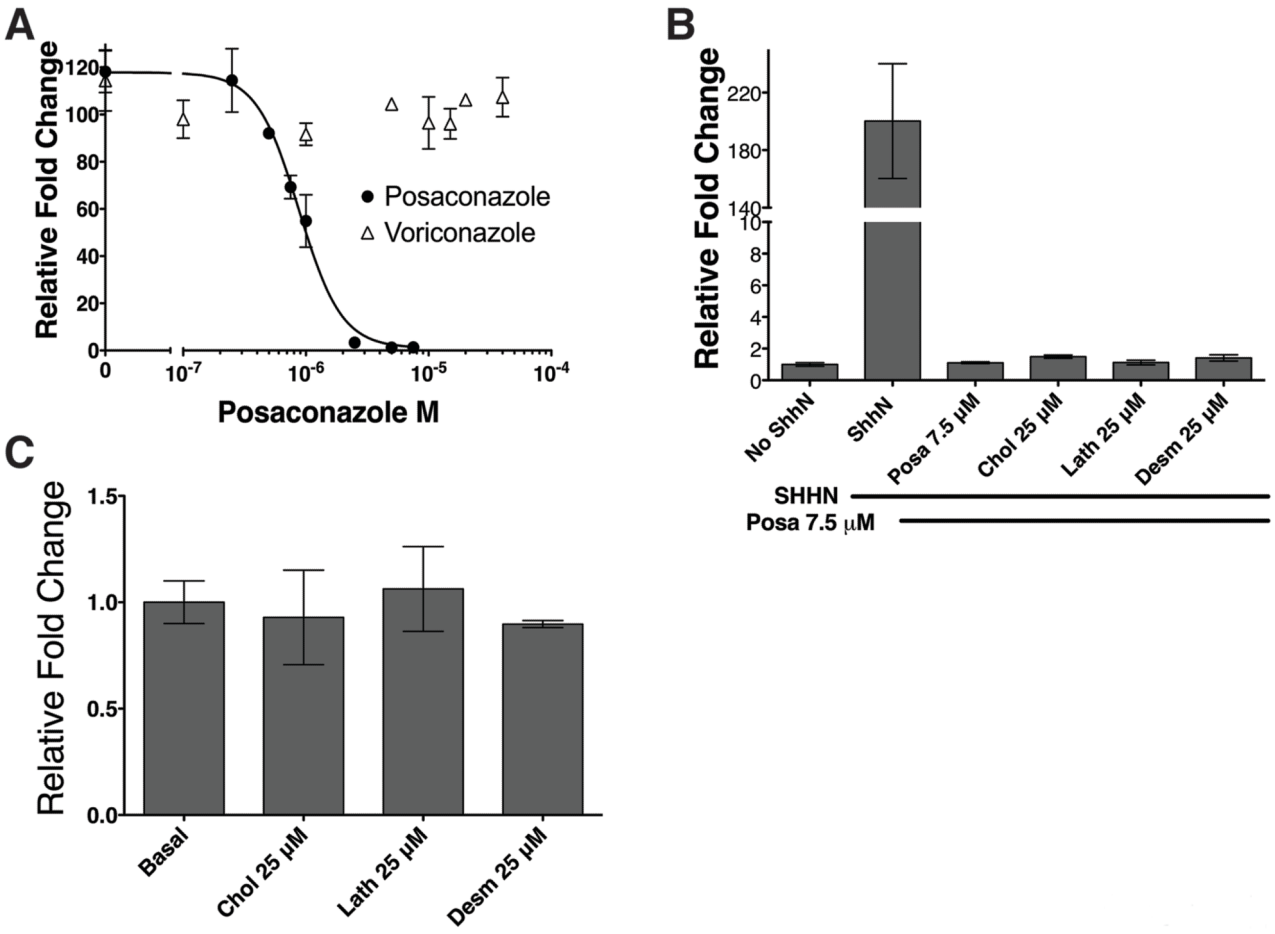

Figure 1. Posaconazole Inhibits The Hedgehog Pathway

8x-Gli binding site luciferase reporter SHH-Light2 cells stimulated with SHHN conditioned medium were used. **(A)** Posaconazole inhibited Hh pathway activation whereas voriconazole, another triazole antifungal drug, did not. **(B)** Inhibition of Hh pathway activation cannot be reversed with the addition of cholesterol, lathosterol, and desmosterol – components of cholesterol biosynthesis downstream of 14α-lanosterol demethylase, the target of posaconazole's antifungal activity. **(C)** Addition of cholesterol, lathosterol, and desmosterol in the absence of SHHN conditioned medium did not induce Hh pathway activity. Data represents mean of triplicates +/- S.D.

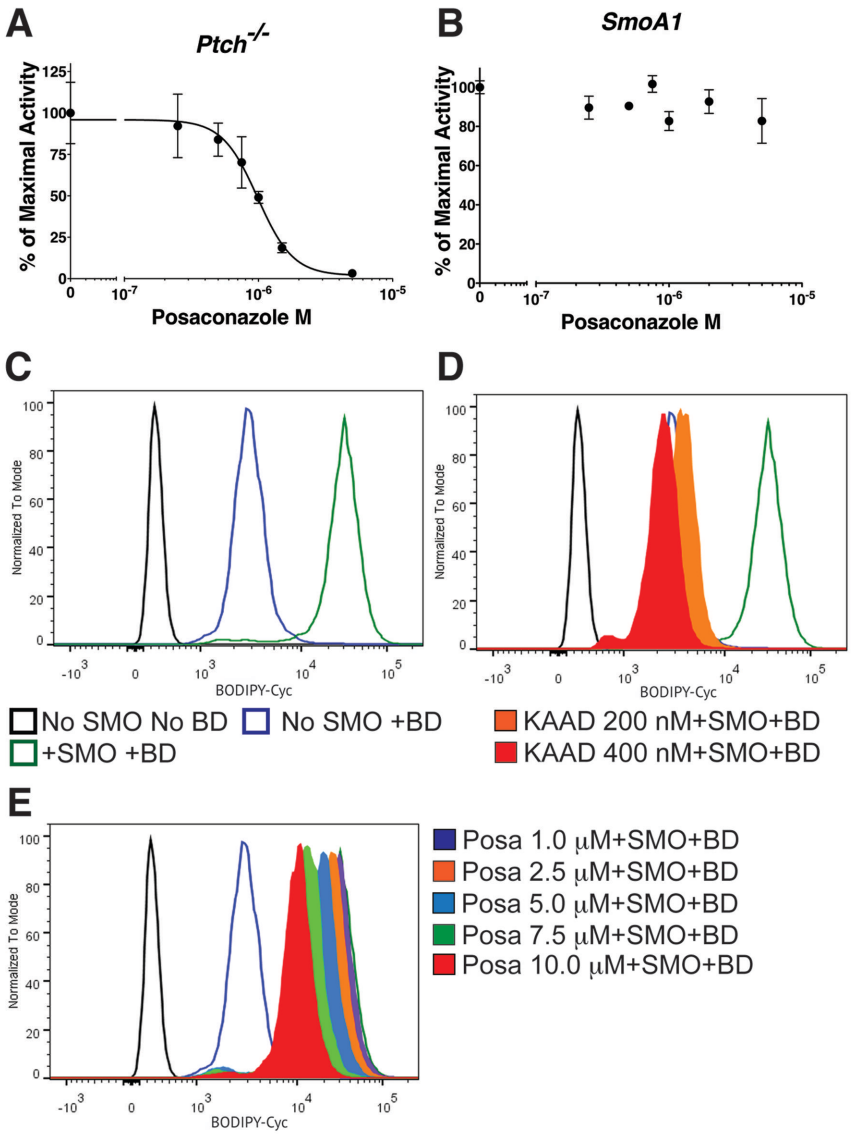

Figure 2. Posaconazole Inhibits the Hh Pathway Downstream Of PTCH

(A) In constitutively active *Ptch*$^{-/-}$ murine fibroblasts transfected with an 8x-Gli luciferase reporter, posaconazole inhibited Hh pathway activity. **(B)** Posaconazole was unable to inhibit the pathway activity of SHH-Light SMOA1 cells stably expressing constitutively active mutant SMOA1. **(C-E)** Histograms of BODIPY-cyclopamine (BD) fluorescence (x-axis), as measured by FACS, using tetracycline-inducible SMO-expressing HEK-293 cells. Graphs are from same experiment separated for clarity. When used, BODIPY-cyclopamine is 5 nM in all panels. **(C)** Black tracing represents uninduced cells (no SMO) with no BODIPY-cyclopamine. Blue trace represents uninduced cells with BODIPY-cyclopamine. Green trace represents maximal fluorescence in cells with induced SMO-overexpression and BODIPY-cyclopamine. **(D)** Addition of KAAD-cyclopamine 200 nM (orange - filled trace; 10x IC_{50}) and 400 nM (red - filled trace; 20x IC_{50}) reduced fluorescence back to baseline

levels. **(E)** Treatment with increasing concentrations of posaconazole up to 10 μM (~11x IC_{50}) did not significantly decrease fluorescence of BODIPY-cyclopamine bound to SMO.

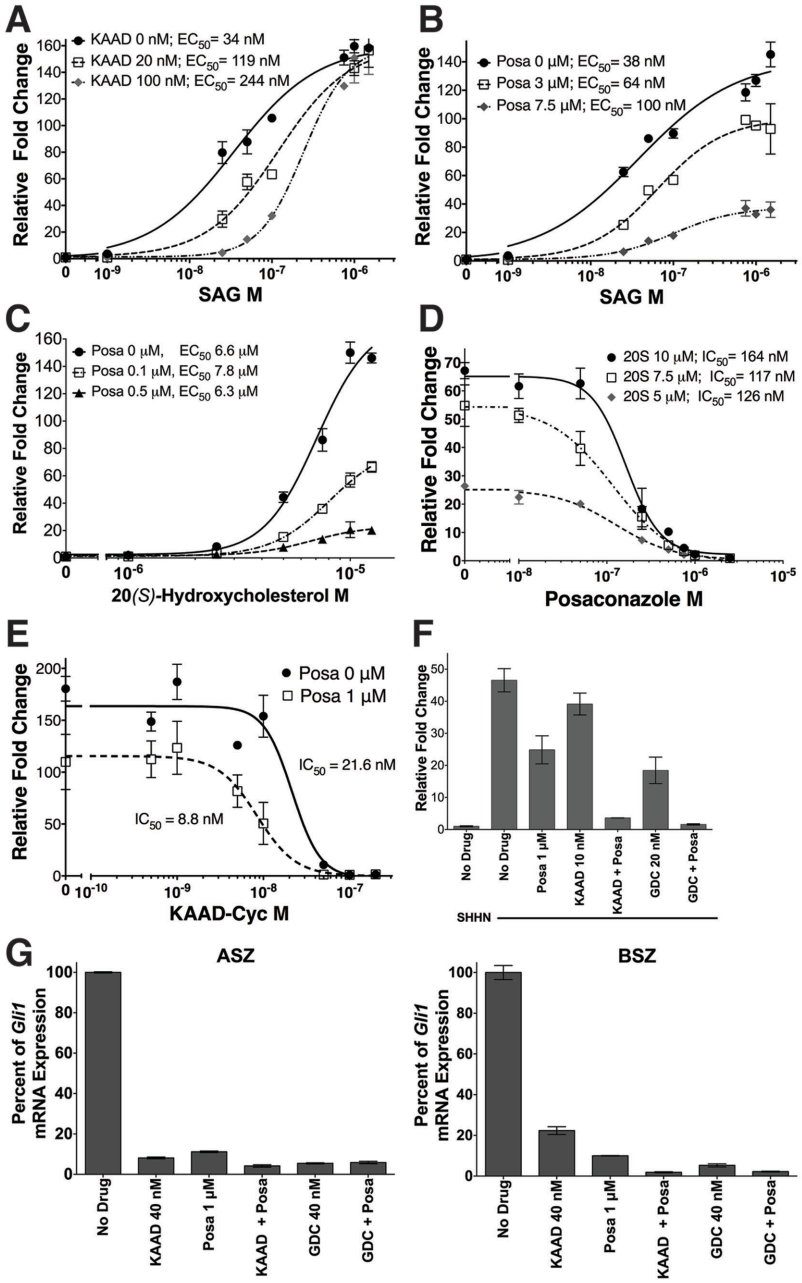

Figure 3. Posaconazole Inhibits The Hh Pathway At Distinct Sites From Other SMO Modulators

Panels A-F represent signaling assays using SHH-Light2 cells stimulated with SAG, a small molecule SMO agonist, or SHHN CM. **(A)** Addition of KAAD-cyclopamine 20 nM (1x IC_{50}) and 100 nM (5x IC_{50}) increased the EC_{50} of SAG ~3.5- and ~7-fold, respectively, while maintaining maximal pathway activation. **(B)** Treatment with posaconazole 1 μM (~1.1 × IC_{50}) and 7.5 μM (~5.5x IC_{50}) decreased the maximal activity of SAG but did not significantly affect its EC_{50}. **(C)** Increasing concentrations of posaconazole while titrating *20(S)*-hydroxycholesterol, an agonist that binds SMO at a distinct site from SAG, decreased maximal pathway activation of *20(S)*-hydroxycholesterol but did not alter its EC_{50}. **(D)**

Increasing concentrations of *20S*-hydroxycholesterol, up to 10 μM, did not significantly alter the IC_{50} of posaconazole. **(E)** The addition of posaconazole caused a reduction in the IC_{50} of KAAD-cyclopamine. **(F)** Treatment with posaconazole 1 μM (~1.1 × IC_{50}), KAAD-cyclopamine 10 nM (~0.5 × IC_{50}) and GDC-0449 20 nM (~1.5 × IC_{50}) partially inhibited Hh pathway activation by SHHN CM. Combination of either KAAD-cyclopamine or GDC-0449 with posaconazole at the same doses further suppressed pathway activation. **(G)** Treatment of ASZ and BSZ, constitutively active murine BCC cells, with posaconazole 1 μM (~1.1 × IC_{50}), KAAD-cyclopamine 40 nM (~2.0 × IC_{50}) and GDC-0449 40 nM (~3.1 × IC_{50}) significantly inhibited the pathway as measured by *Gli1* mRNA. Combination of posaconazole with either KAAD-cyclopamine or GDC-0449 completely inhibited pathway activity. For panels A-E, respective IC_{50} or EC_{50} of the titrated compound under varying conditions are listed in the figure. All data represents mean of triplicates +/- S.D.

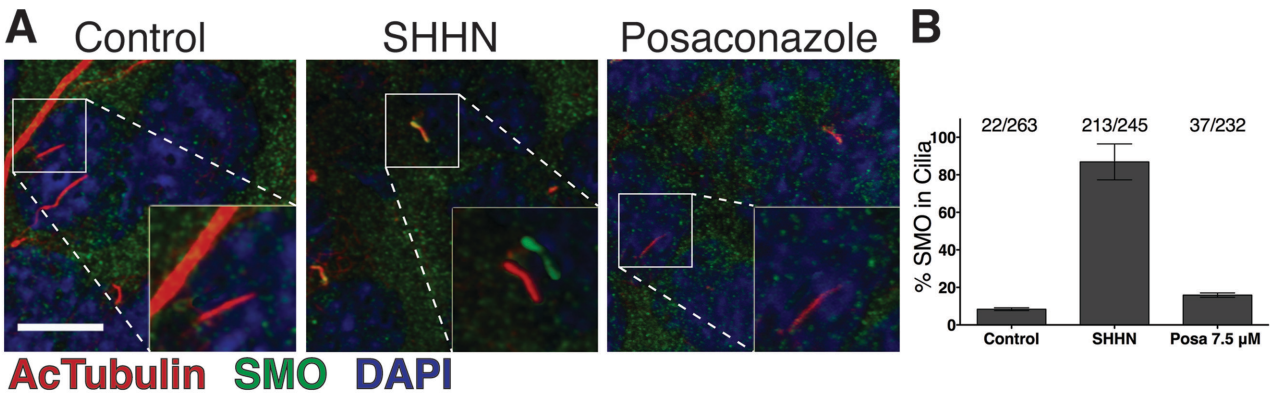

Figure 4. Posaconazole Inhibits SMO Accumulation In Primary Cilia

(A) Representative immunofluorescent images of NIH-3T3 cells. Stimulation of Hh pathway with SHHN led to accumulation of SMO in primary cilia. Treatment of posaconazole 7.5 μM with SHHN inhibited SMO accumulation in primary cilia. Insets show enlarged views of boxed primary cilia with acetylated tubulin (red) and SMO (green) channels offset for clarity. **(B)** Tabulation of SMO accumulation in primary cilia. Data represent mean of at least 7 fields +/- S.D. Scale bar represents 10 μm.

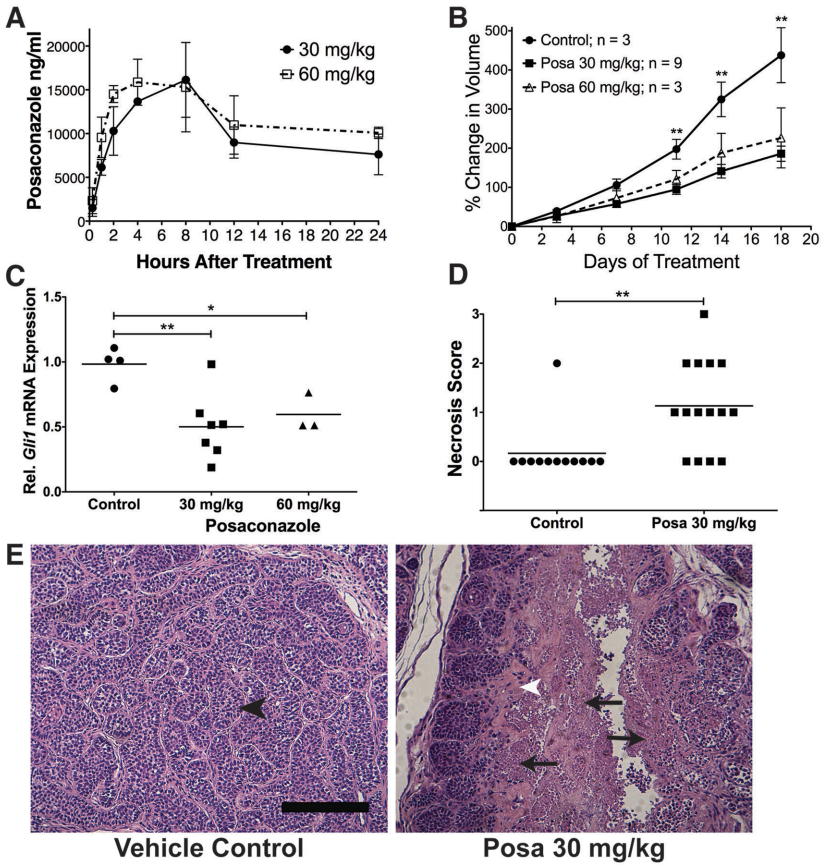

Figure 5. In Vivo Treatment With Posaconazole

(A) Plasma Pharmacokinetics of Posaconazole. Balb-c mice were treated with one dose of posaconazole and plasma levels of posaconazole were measured at various time points after treatment. Each data point represents mean of 3 mice +/- S.D. **(B)** Posaconazole treatment of nude mice bearing subcutaneous allografts of murine *Ptch*$^{+/-}$;*p53*$^{-/-}$ basal cell carcinomas suppressed tumor growth compared to vehicle control. '**' $p < 0.005$. **(C)** Posaconazole treatment decreased Hh pathway activation in allografted basal cell carcinomas compared to vehicle control treated tumors, as measured by *Gli1* mRNA levels. *Gli1* mRNA levels of posaconazole treated tumors were normalized to the mean of vehicle treated tumors. Treatments were given twice per day by oral gavage for 5 days. Line represents mean of data sets.'*' $p = 0.0224$, '**' $p = 0.0033$ **(D and E)** BCC tumors treated with posaconazole showed increased tumor necrosis compared to control vehicle. **(D)** Tabulation of necrosis scores of tumors (see Methods). Line represents mean of data set. '**' $p = 0.0028$. **(E)** Representative images of BCC treated with vehicle control and posaconazole 30 mg/kg. Vehicle control treated tumors showed structured and ordered nests of tumor cells surrounded by stroma (black arrowhead). In contrast, posaconazole treated tumors showed destruction of organized tumor epithelial architecture (arrow) with increased stroma (white arrowhead). Scale bar represents 200 μm.

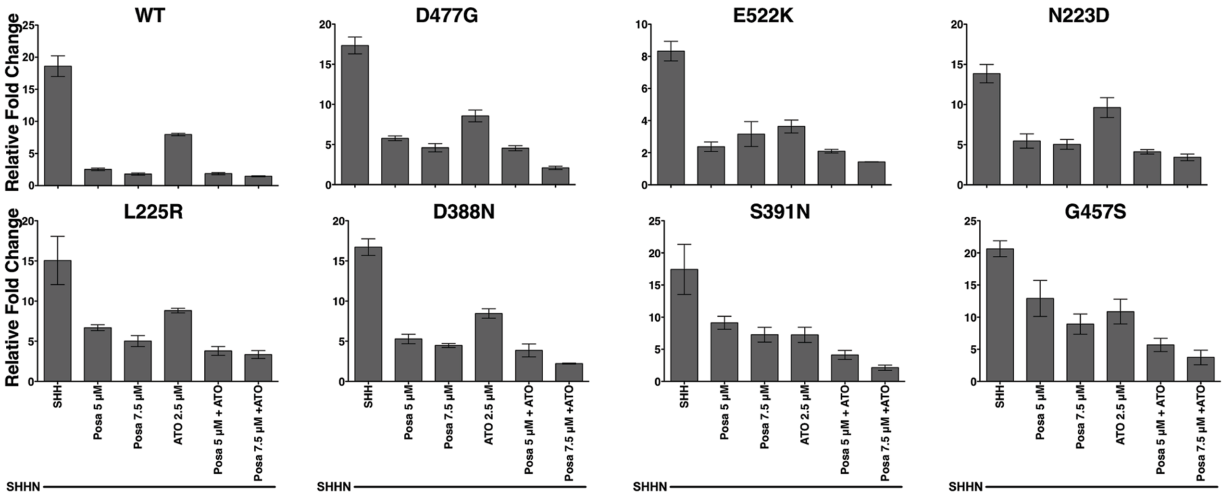

Figure 6. Posaconazole and ATO Inhibit the Activity of Drug-resistant SMO Mutants

Signaling assays of *Smo*$^{-/-}$ fibroblasts transfected with 8x-Gli luciferase reporter and either wild-type or mutant Smo constructs resistant to vismodegib (GDC-0449) or sonidegib (LDE225) and stimulated with SHHN CM. Posaconazole, ATO or combination inhibited the drug-resistant mutant SMO activity. SMO D477G and E522K are vismodegib-resistant. All other SMO mutants are resistant to sonidegib. “WT” = Wild Type. Data represents mean of triplicates +/- S.D.